AN EXPLICIT FINITE ELEMENT METHOD FOR DYNAMIC ANALYSIS IN FLUID SATURATED POROUS MEDIA CONSIDERING THE COUPLING MASS*

Chenggang Zhao, Weihua Li, liang Dong, Xuedong Zhang
School of Civil Engineering and Architecture, Beijing JiaoTong University, Beijng 100044
Email: cgzhaot@bjtu.edu.cn

ABSTRACT
Based on Biot dynamic theory, an explicit finite element method for dynamic analysis of the fluid saturated porous media was proposed considering of the coupling massρ_a. The formula of the explicit finite element method was developed, and the corresponding calculation procedure and some results were presented in this paper. The excellent characteristics of the method are that the global stiffness matrix does not need to be assembled and the linear equations do not need to be solved. So the computational effort and memory requirement can be reduced considerably. Compared with the analytic solution, the results were in a good conformity with it, which indicated that the method presented in this paper was an effective method to deal with the dynamic problems of saturated porous media. The effects of coupling massρ_a on the displacements of liquid and solid phase were also analyzed, and the results showed that the coupling mass had obvious effects on the displacements of liquid phase, but not obvious on the solid phase's displacements.
KEYWORDS: Fluid saturated porous media; Explicit finite element method; Boit dynamic equation; Coupling massρ_a

1. INTRODUCTION

How to solve and analyze the dynamic response of a structure in the earth and a site with saturated porous media is important in earthquake engineering and soil dynamics. Biot [1] (1956) developed the propagation theory of elastic waves in fluid-saturated porous media. Biot's work is a milestone that sets the foundation to solve and analyze the mentioned-above problems. Complicated equations given in Biot dynamic theory can be solved by analytical methods only with some simple boundary conditions. Most dynamic problems in fluid-saturated porous media are solved using numerical methods, especially using finite element methods. Ghaboussi et al [2], Zienkiewicz et al [3, 4], Prevost[5], Aubry[6], Yuan et al [7] and others have developed the finite element methods applied to the dynamic problems in fluid-saturated porous media. If the implicit finite element methods are used in the time domain, there is a disadvantage in them, which require dividing time into time steps and solving a set of linear equations within each time step. These methods are quite suitable when problems are with a few degrees of freedom. For problems with a large number of degrees of freedom, the computational effort and memory requirement will be increased enormously, so the application of these methods to practical problems is limited. To overcome the disadvantage of these methods, an explicit finite element method for Biot dynamic formulation in fluid-saturated porous media is developed by Z.Chenggang et al [8, 9]. The excellent characteristics of the method are that the global stiffness matrix does not need to be assembled and the linear equations do not need to be solved, so the computational effort and memory requirement can be reduced considerably. But the method does not consider the effect of the coupling masspa in Biot dynamic theory. In this paper, the method [8] was further developed, and the new formula are produced in which the effect of the coupling masspa is considered. The excellent characteristics of the above mentioned method [8] are kept.

The corresponding calculation procedures and some results were presented. Compared with the analytic solution, the results were in a good conformity with it, which indicated that the method presented in this paper was an effective method to deal with the dynamic problems of saturated porous media. The effects of coupling masspa on the displacements of liquid and solid phase were also analyzed, and the results showed that the coupling mass had obvious effects on the displacements of liquid phase, but not obvious on the displacements of solid phase.

2. ESTABLISHMENT OF EXPLICIT FINITE ELEMENT EQUATIONS

The dynamic equations for fluid saturated porous media established by Biot[1] can be given by aligned matrix.

$$\begin{cases} [L]^T[D_1][L]\{\boldsymbol{u}\}+[L]^T[D_2][L]\{\boldsymbol{U}\}=\rho_{11}\{\ddot{\boldsymbol{u}}\}+b\ (\{\dot{\boldsymbol{u}}\}-\{\dot{\boldsymbol{U}}\}) \\ [L]^T[D_2][L]^T\{\boldsymbol{u}\}+[L]^T[D_3][L]\{\boldsymbol{U}\}=\rho_{22}\{\ddot{\boldsymbol{U}}\}-b\ (\{\dot{\boldsymbol{u}}\}-\{\dot{\boldsymbol{U}}\}) \end{cases} \tag{2.1}$$

Where: $[L]^T=\begin{bmatrix} \frac{\partial}{\partial x} & 0 & \frac{\partial}{\partial y} \\ 0 & \frac{\partial}{\partial y} & \frac{\partial}{\partial x} \end{bmatrix}$; $\{\boldsymbol{u}\}=\begin{Bmatrix} u_x \\ u_y \end{Bmatrix}$; $\{\boldsymbol{U}\}=\begin{Bmatrix} U_x \\ U_y \end{Bmatrix}$; $[D_1]=\begin{bmatrix} A+2N & A & 0 \\ A & A+2N & 0 \\ 0 & 0 & N \end{bmatrix}$; $[D_2]=\begin{bmatrix} Q & Q & 0 \\ Q & Q & 0 \\ 0 & 0 & 0 \end{bmatrix}$;

$[D_3]=\begin{bmatrix} R & R & 0 \\ R & R & 0 \\ 0 & 0 & 0 \end{bmatrix}$.

With $\boldsymbol{u}$ and $\boldsymbol{U}$ are the displacements of solid phase and liquid phase respectively, $\rho_{11}=\rho_1+\rho_a$; $\rho_{22}=\rho_2+\rho_a$; $\rho_{12}=-\rho_a$; and $\rho_1=(1-n)\rho_s$; $\rho_2=n\rho_f$, ρ_s is the density of solid mass, ρ_f is the density of liquid mass, ρ_a is the density of coupled-mass between solid phase and liquid phase. The coefficient b is relative to permeability, $b=\zeta n^2/k$; ζ represents the coefficient of fluid viscosity, n represents porosity, and k represents the coefficient of permeability. N and A are similar to Lame constants μ and λ in elastic theory. R and Q are obtained by experiments. Biot presented all above parameters in detail.

2.1 Establishment of the aligned finite equation

According to the Ref [4,8], the Galerkin weak form of the dynamic equation could be directly given by matrix form as follows (where,$\rho_{12}\neq 0$).

$$\begin{aligned} &\sum_e\int_{\Omega^e}[N]^T\rho_{11}[N]\{\ddot{u}_e\}dxdy+\sum_e\int_{\Omega^e}[N]^T\rho_{12}[N]\{\ddot{U}_e\}dxdy+\sum_e\int_{\Omega^e}[N]^Tb[N](\{\dot{u}_e\}-\{\dot{U}_e\})dxdy+\sum_e\int_{\Omega^e}[B]^T[D_{11}][B]\{u_e\}dxdy \\ &+\sum_e\int_{\Omega^e}[B]^T[D_{12}][B]\{U_e\}dxdy=\sum_e\oint_{\Gamma^e}[N]^T\{f_{u_e}\}d\Gamma \\ &\sum_e\int_{\Omega^e}[N]^T\rho_{12}[N]\{\ddot{u}_e\}dxdy+\sum_e\int_{\Omega^e}[N]^T\rho_{22}[N]\{\ddot{U}_e\}dxdy-\sum_e\int_{\Omega^e}[N]^Tb[N](\{\dot{u}_e\}-\{\dot{U}_e\})dxdy+\sum_e\int_{\Omega^e}[B]^T[D_{12}][B]\{u_e\}dxdy \\ &+\sum_e\int_{\Omega^e}[B]^T[D_{13}][B]\{U_e\}dxdy=\sum_e\oint_{\Gamma^e}[N]^T\{f_{U_e}\}d\Gamma \end{aligned} \tag{2.2}$$

Where, [N] is the shape function of the element; $\{u_e\}$, $\{U_e\}$ and $\{f_{u_e}\}$, $\{f_{U_e}\}$represent the nodal displacements and the nodal forces of solid and liquid phases in the element e respectively.

2.2 Meshing

The plane area Ω is divided into *m* linear quadrilateral elements and *k* nodes altogether. The displacements and boundary force of solid and liquid phase of 4 nodes in element *e* can be described as follows:

$$\left.\begin{aligned} &\{u_e\}^T=\begin{bmatrix}u_1^T & u_2^T & u_3^T & u_4^T\end{bmatrix}\\ &u_i^T=\begin{bmatrix}u_{ix} & u_{iy}\end{bmatrix}\\ &\{U_e\}^T=\begin{bmatrix}U_1^T & U_2^T & U_3^T & U_4^T\end{bmatrix}\\ &U_i^T=\begin{bmatrix}U_{ix} & U_{iy}\end{bmatrix}\end{aligned}\right\}(i=1,2,3,4),\quad \left.\begin{aligned} &\{f_{u_e}\}^{\mathrm{T}}=\begin{bmatrix}f_{u_1} & f_{u_2} & f_{u_3} & f_{u_4}\end{bmatrix}\\ &f_{u_i}{}^{\mathrm{T}}=\begin{bmatrix}f_{u_{ix}} & f_{u_{iy}}\end{bmatrix}\\ &\{f_{U_e}\}^{\mathrm{T}}=\begin{bmatrix}f_{U_1} & f_{U_2} & f_{U_3} & f_{U_4}\end{bmatrix}\\ &f_{U_i}{}^{\mathrm{T}}=\begin{bmatrix}f_{U_{ix}} & f_{U_{iy}}\end{bmatrix}\end{aligned}\right\}(i=1,2,3,4) \tag{2.3}$$

Where, u_{ix}, u_{iy}, U_{ix} and U_{iy} are lateral and longitudinal displacements of solid and liquid phase of node *i* in element e, respectively, and $f_{u_{ix}}$, $f_{u_{iy}}$, $f_{U_{ix}}$ and $f_{U_{iy}}$ are the lateral and longitudinal boundary force of solid and liquid phase of node *i* in element e, respectively.

The physical quantities of a certain node can be expressed by that of the adjacent notes, namely only the adjacent nodes have effects on it. "*L*" represents the influence of various elements on node *i*, only four elements' calculation results are provided because only they enclose the node *i* and have effects on it. "*j*" represents the influence of 4 nodes in one element, shown as Fig. 1.

2.3 Discrete equations and decoupling technique

Accuracy of numerical simulation on wave problems requires that the size of finite element should be small enough comparing with wavelength, so the inertia force in every element change little, and they are assumed constant in the same element, then the acceleration of the element can be assumed constant, namely it is equal to the nodal acceleration ($\ddot{u}_j^e=\ddot{u}_i$), therefore mass matrix can be decoupled and Eq.2 can be turned into the following form:

$$\left.\begin{aligned} &\sum_{L=1}^{4}\sum_{j=1}^{4}M_{uij}^L\ddot{u}_j^L+\sum_{L=1}^{4}\sum_{j=1}^{4}\tilde{M}_{uUij}^L\ddot{U}_j^L+\sum_{L=1}^{4}\sum_{j=1}^{4}C_{ij}^L\left(\dot{u}_j^L-\dot{U}_j^L\right)+\\ &\sum_{L=1}^{4}\sum_{j=1}^{4}K_{uuij}^Lu_j^L+\sum_{L=1}^{4}\sum_{j=1}^{4}K_{uUij}^LU_j^L=\sum_{L=1}^{4}f_{ui}^L\\ &\sum_{L=1}^{4}\sum_{j=1}^{4}\tilde{M}_{uUij}^L\ddot{u}_j^L+\sum_{L=1}^{4}\sum_{j=1}^{4}M_{Uij}^L\ddot{U}_j^L-\sum_{L=1}^{4}\sum_{j=1}^{4}C_{ij}^L\left(\dot{u}_j^L-\dot{U}_j^L\right)+\\ &\sum_{L=1}^{4}\sum_{j=1}^{4}K_{Uuij}^Lu_j^L+\sum_{L=1}^{4}\sum_{j=1}^{4}K_{UUij}^LU_j^L=\sum_{L=1}^{4}f_{Ui}^L\end{aligned}\right\} \tag{2.4}$$

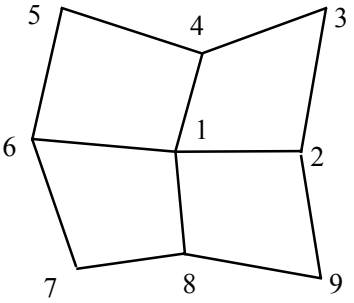

Fig. 1 The local nodes system

with

$$M_{ui}\ddot{u}_i=\sum_{L=1}^{4}\sum_{j=1}^{4}M_{uij}^L\ddot{u}_j^L;\quad M_{Ui}\ddot{U}_i=\sum_{L=1}^{4}\sum_{j=1}^{4}M_{Uij}^L\ddot{U}_j^L;\quad \tilde{M}_{uUi}\ddot{u}_i=\sum_{L=1}^{4}\sum_{j=1}^{4}\tilde{M}_{uUij}^L\ddot{u}_j^L$$

and where

$$M_{uij}^L=\iint_{\Omega^L}\rho_{11}[N_i][N_j]dxdy=\int_{-1}^{1}\int_{-1}^{1}\rho_{11}[N_i][N_j]J|d\xi d\eta;\ M_{Uij}^L=\iint_{\Omega^L}\rho_{22}[N_i][N_j]dxdy=\int_{-1}^{1}\int_{-1}^{1}\rho_{22}[N_i][N_j]J|d\xi d\eta$$

$$\tilde{M}_{uUij}^L=\iint_{\Omega^L}\rho_{12}[N_i][N_j]dxdy=\int_{-1}^{1}\int_{-1}^{1}\rho_{12}[N_i][N_j]J|d\xi d\eta;\ C_{ij}^L=\iint_{\Omega^L}b[N_i][N_j]dxdy=\int_{-1}^{1}\int_{-1}^{1}b[N_i][N_j]J|d\xi d\eta$$

$$K_{uuij}^L=\int_{-1}^{1}\int_{-1}^{1}[B_i]^T[D_{11}][B_j]J|d\xi d\eta;\quad K_{Uuij}^L=K_{uUij}^L=\int_{-1}^{1}\int_{-1}^{1}[B_i]^T[D_{12}][B_j]J|d\xi d\eta;\quad f_{ui}^L=\int_{-L}[N_i]\tilde{T}_s dr$$

$$K_{UUij}^L=\int_{-1}^{1}\int_{-1}^{1}[B_i]^T[D_{13}][B_j]J|d\xi d\eta;\quad f_{Ui}^L=\int_{-L}[N_i]\begin{Bmatrix}np\\np\end{Bmatrix}dr;\qquad \tilde{T}_s=\begin{Bmatrix}\tilde{T}_x\\\tilde{T}_y\end{Bmatrix}.$$

in which, $\widetilde{T}_x$ and $\widetilde{T}_y$ are the lateral and longitudinal distributing force of solid phase in L element boundary, respectively; p is the boundary pore water pressure.

2.4 Dynamic response expressions of internal nodes

When finite element method is used to deal with an infinite extent question, artificial boundaries have to be introduced, so the nodes in finite element grids should be divided into artificial boundary nodes and internal nodes. The dynamic response expressions of artificial boundary nodes can be represented by those of the internal nodes and input movement, which will be stated later (see artificial boundary).

The motion equations of inside nodes can be gained as follows according to Eq. (2.4), where Δt is the time step, p is amount of steps.

$$\left.\begin{aligned} M_{ui}\ddot{u}_i^p+\widetilde{M}_{uUi}\ddot{U}_i^p+\sum_{L=1}^{4}\sum_{j=1}^{4}C_{ij}^{L}\left(\dot{u}_j^{L,p}-\dot{U}_j^{L,p}\right)+\sum_{L=1}^{4}\sum_{j=1}^{4}K_{uuij}^{L}u_j^{L,p}+\sum_{L=1}^{4}\sum_{j=1}^{4}K_{uUij}^{L}U_j^{L,p}=\sum_{L=1}^{4}f_{ui}^{L,p}\\ \widetilde{M}_{uUi}\ddot{u}_i^p+M_{Ui}\ddot{U}_i^p-\sum_{L=1}^{4}\sum_{j=1}^{4}C_{ij}^{L}\left(\dot{u}_j^{L,p}-\dot{U}_j^{L,p}\right)+\sum_{L=1}^{4}\sum_{j=1}^{4}K_{Uuij}^{L}u_j^{L,p}+\sum_{L=1}^{4}\sum_{j=1}^{4}K_{UUij}^{L}U_j^{L,p}=\sum_{L=1}^{4}f_{Ui}^{L,p}\end{aligned}\right\} \tag{2.5}$$

Through central difference method in time domain, we get the following equations:

$$\left\{\dot{W}_i^p\right\}=\frac{1}{2\Delta t}\left(\left\{W_i^{p+1}\right\}-\left\{W_i^p\right\}\right),\quad \left\{\ddot{W}_i^p\right\}=\frac{1}{\Delta t^2}\left(\left\{W_i^{p+1}\right\}-2\left\{W_i^p\right\}+\left\{W_i^{p-1}\right\}\right) \tag{2.6}$$

then

$$\left\{\ddot{W}_i^p\right\}=\frac{2}{\Delta t^2}\left(\left\{W_i^{p+1}\right\}-\left\{W_i^p\right\}\right)-\frac{2}{\Delta t}\left\{\dot{W}_i^p\right\} \tag{2.7}$$

Where $\left\{W_i^q\right\}$, $\left\{\dot{W}_i^q\right\}$ and $\left\{\ddot{W}_i^q\right\}$represent the displacement, velocity and acceleration of the node i at the time step q respectively. For simplifying expression, W=u, U; q=p-1, p , p +1, q and p all present time steps.

The assumption for New-mark constant average acceleration method is given as follows:

$$\frac{\left\{\ddot{W}_i^{p+1}\right\}+\left\{\ddot{W}_i^p\right\}}{2}=\frac{\left\{\dot{W}_i^{p+1}\right\}-\left\{\dot{W}_i^p\right\}}{\Delta t},\quad \frac{\left\{\dot{W}_i^{p+1}\right\}+\left\{\dot{W}_i^p\right\}}{2}=\frac{\left\{W_i^{p+1}\right\}-\left\{W_i^p\right\}}{\Delta t} \tag{2.8}$$

Introducing the expression of Eq. (2.6)-(2.8) into Eq. (2.5), we can obtain:

$$\begin{aligned} u_i^{p+1}=&u_i^p+\Delta t\dot{u}_i^p-\frac{\Delta t^2}{2}\left(M_{ui}-\frac{\widetilde{M}_{uUi}\widetilde{M}_{uUi}}{M_{Ui}}\right)^{-1}\left\{\left(\sum_{L=1}^{4}\sum_{j=1}^{4}C_{ij}^{l}\left(\dot{u}_j^{L,p}-\dot{U}_j^{L,p}\right)\left(1+\frac{\widetilde{M}_{uUi}}{M_{Ui}}\right)\right)\right.\\ &\left.+\left(\sum_{L=1}^{4}\sum_{j=1}^{4}K_{uuij}^{L}u_j^{L,p}\right)+\left(\sum_{L=1}^{4}\sum_{j=1}^{4}K_{uUij}^{L}U_j^{L,p}\right)-\left(\sum_{L=1}^{4}\sum_{j=1}^{4}K_{uUij}^{L}u_j^{L,p}\frac{\widetilde{M}_{uUi}}{M_{Ui}}\right)-\left(\sum_{L=1}^{4}\sum_{j=1}^{4}K_{UUij}^{L}U_j^{L,p}\frac{\widetilde{M}_{uUi}}{M_{Ui}}\right)-\sum_{L=1}^{4}f_{ui}^{L,p}+\sum_{L=1}^{4}f_{Ui}^{L,p}\frac{\widetilde{M}_{uUi}}{M_{Ui}}\right\}\end{aligned} \tag{2.9}$$

$$\begin{aligned} U_i^{p+1}=&U_i^p+\Delta t\dot{U}_i^p-\frac{\Delta t^2}{2}\left(M_{Ui}-\frac{\widetilde{M}_{uUi}\widetilde{M}_{uUi}}{M_{ui}}\right)^{-1}\left\{\left(\sum_{L=1}^{4}\sum_{j=1}^{4}C_{ij}^{l}\left(\dot{u}_j^{L,p}-\dot{U}_j^{L,p}\right)\left(-1-\frac{\widetilde{M}_{uUi}}{M_{ui}}\right)\right)\right.\\ &\left.-\left(\sum_{L=1}^{4}\sum_{j=1}^{4}K_{uuij}^{L}u_j^{L,p}\frac{\widetilde{M}_{uUi}}{M_{ui}}\right)-\left(\sum_{L=1}^{4}\sum_{j=1}^{4}K_{uUij}^{L}U_j^{L,p}\frac{\widetilde{M}_{uUi}}{M_{ui}}\right)+\left(\sum_{L=1}^{4}\sum_{j=1}^{4}K_{uUij}^{L}u_j^{L,p}\right)+\left(\sum_{L=1}^{4}\sum_{j=1}^{4}K_{UUij}^{L}U_j^{L,p}\right)-\sum_{L=1}^{4}f_{Ui}^{L,p}+\sum_{L=1}^{4}f_{ui}^{L,p}\frac{\widetilde{M}_{uUi}}{M_{ui}}\right\}\end{aligned} \tag{2.10}$$

$$\begin{aligned} \dot{u}_i^{p+1}=&\dot{u}_i^p-\left(M_{ui}-\frac{\widetilde{M}_{uUi}\widetilde{M}_{uUi}}{M_{Ui}}\right)^{-1}\left\{\left(\sum_{L=1}^{4}\sum_{j=1}^{4}C_{ij}^{l}\left(u_j^{L,p+1}-u_j^{L,p}-U_j^{L,p+1}+U_j^{L,p}\right)\left(1+\frac{\widetilde{M}_{uUi}}{M_{Ui}}\right)\right)+\frac{\Delta t}{2}\left[\left(\sum_{L=1}^{4}\sum_{j=1}^{4}K_{uuij}^{l}\left(u_j^{L,p+1}+u_j^{L,p}\right)\right)+\left(\sum_{L=1}^{4}\sum_{j=1}^{4}K_{uUij}^{L}\left(U_j^{L,p+1}+U_j^{L,p}\right)\right)-\right.\right.\\ &\left.\left.\left(\sum_{L=1}^{4}\sum_{j=1}^{4}K_{uUij}^{L}\left(u_j^{L,p+1}+u_j^{L,p}\right)\frac{\widetilde{M}_{uUi}}{M_{Ui}}\right)-\left(\sum_{L=1}^{4}\sum_{j=1}^{4}K_{UUi}^{L}\left(U_j^{L,p+1}+U_j^{L,p}\right)\frac{\widetilde{M}_{uUi}}{M_{Ui}}\right)-\sum_{L=1}^{4}\left(f_{ui}^{L,p+1}+f_{ui}^{L,p}\right)+\sum_{L=1}^{4}\left(f_{Ui}^{L,p+1}+f_{Ui}^{L,p}\right)\frac{\widetilde{M}_{uUi}}{M_{Ui}}\right]\right\}\end{aligned} \tag{2.11}$$

$$\dot{U}_i^{p+1}=\dot{U}_i^p-\left(M_{Ui}-\frac{\widetilde{M}_{uUi}\widetilde{M}_{uUi}}{M_{ui}}\right)^{-1}\left\{\left(\sum_{L=1}^{4}\sum_{j=1}^{4}C_{ij}^{L}\left(u_j^{L,p+1}-u_j^{L,p}-U_j^{L,p+1}+U_j^{L,p}\right)\left(-1-\frac{\widetilde{M}_{uUi}}{M_{ui}}\right)\right)+\frac{\Delta t}{2}\left[\left(\sum_{L=1}^{4}\sum_{j=1}^{4}K_{uUij}^{L}\left(u_j^{L,p+1}+u_j^{L,p}\right)\right)+\left(\sum_{L=1}^{4}\sum_{j=1}^{4}K_{UUij}^{L}\left(U_j^{L,p+1}+U_j^{L,p}\right)\right)-\left(\sum_{L=1}^{4}\sum_{j=1}^{4}K_{uuij}^{L}\left(u_j^{L,p+1}+u_j^{L,p}\right)\frac{\widetilde{M}_{uUi}}{M_{ui}}\right)-\left(\sum_{L=1}^{4}\sum_{j=1}^{4}K_{uUi}^{L}\left(U_j^{L,p+1}+U_j^{L,p}\right)\frac{\widetilde{M}_{uUi}}{M_{ui}}\right)-\sum_{L=1}^{4}\left(f_{Ui}^{L,p+1}+f_{Ui}^{L,p}\right)+\sum_{L=1}^{4}\left(f_{ui}^{L,p+1}+f_{ui}^{L,p}\right)\frac{\widetilde{M}_{uUi}}{M_{ui}}\right]\right\} \tag{2.12}$$

The expression for acceleration can be obtained from Eq. (2.8):

$$\ddot{u}_i^{p+1}=-\ddot{u}_i^p+2\left(\dot{u}_i^{p+1}-\dot{u}_i^p\right)/\Delta t;\qquad \ddot{U}_i^{p+1}=-\ddot{U}_i^p+2\left(\dot{U}_i^{p+1}-\dot{U}_i^p\right)/\Delta t \tag{2.13}$$

Therefore, according to Eqns. (2.9)-(2.13), the dynamic response of a certain time can be obtained through the response of former time.

3 . ARTIFICIAL BOUNDARY

There are three types of wave (P_I; P_{II} and S waves) in a fluid-saturated porous media according to Biot dynamic theory. Each type of wave propagates at an inherent velocity, That is to say, (such as P_I wave) for a specific type of wave no matter it is solid or liquid phase, both of them propagate at the same velocity to the same direction, but there is a fixed relationship between them. Based on the transmitting artificial boundary theory [10], we postulate that the propagation of both solid and liquid phase passes through artificial boundaries at the same velocity to the same direction. So we use transmitting artificial boundary formulae to both solid and liquid phase separately, and in this way the scattering wave fields of both solid and liquid phase along artificial boundary nodes can be calculated.

4. CALCULATION PROCEDURES

The calculation procedure of dynamic response utilizing explicit finite element method is established by this paper can be summarized as follows:

1) Introducing the artificial boundary and providing calculation area.

2) Inputting initial displacement field or the initial applied force field.

3) Dividing the area into finite element mesh, the continuum area will be replaced with the finite element node system.

4) Preparation for calculation

□ Forming the mass concentrated on every node;

□ Forming calculation rigidity and damping in every node;

□ Letting the nodal displacement of p=0 and several moments before p =0 be zero.

5) Calculating the node external forces in time step p and p +1.

6) Calculating the dynamic response in time step p +1

□ Calculating dynamic response displacements for every internal nodes at $t+\Delta t$ (in the time step p+1) by using Eq.12 and Eq.13, and combing $u_s=u-u_I$ (u_I is the incidence displacement field)， one can get the artificial boundary scattering displacement field and calculate the scattering displacement in time step p+1 at the artificial boundary, then utilizing $u=u_s+u_I$ one can obtain the total displacement field at the artificial boundary.

□It is by means of Eq.14 and Eq. 15 that the speed response can be calculated at the $t+\Delta t$ (in the time step p+1) for every internal nodes, the same as procedure □ of step 6) one can obtain the total velocity field at the

artificial boundary.

Calculating the acceleration response of every internal nodes at $t+\Delta t$ (in the time step p+1) with the Eq. 15, the same as the procedure of step 6) one can obtain the total velocity field at artificial boundary.

7) Circulation steps 5) and 6) can be used to calculate the dynamic response of all the nodes at different time on the computational gridding.

5. EXAMPLES

Example 1

An explicit finite element method for dynamic analysis of fluid saturated porous media was presented above, now the corresponding procedure are worked out by using the formula deduced above and the instance analysis are carried on.

In order to prove the accuracy of the method presented in this paper, the dynamic response of the system shown in Fig. 2 is calculate by both the analytic method according to Ref [12] and the method present in this paper. In Fig.2, the analytic models and the situation after utilizing the method of this paper to introduce the artificial boundary are illustrated (Meshing is not needed for analytic model), the lateral and vertical calculated ranges of the model both are 200m, the interval Δx and vertical interval Δy are 2.5m respectively, the model is divided into 6400 units and 6561 nodes altogether, the node loads P=1 are exerted on the mid point of the free surface, the free surface can be permeable or impermeable. When the free surface is permeable, the pore water pressure on it is zero, and when the free surface is impermeable, the vertical displacements of the solid phase and that of the liquid phase on it are equal. In this example, the permeable surface condition is discussed. The material characteristic parameter is presented in Table 1. The numerical results and analytic solutions are compared as follow.

When the free surface is permeable, the numerical solution and analytic solution of the solid phase displacements of point B with ρ_a=0.0877×10^4 are presented in Fig.3[0], with $\tau = t/\rho k$ (ρ is the total density of fluid saturated porous media, k is permeability coefficient) being the horizontal axis, and $\xi = u/\rho k V_c$ (V_c is dilatational wave velocity of fluid saturated porous media without relative motion between fluid and solid)being the vertical axis, respectively. From Fig.3 we can find out that they are in good coincidence, which indicate that the method presented in this paper has satisfied accuracy.

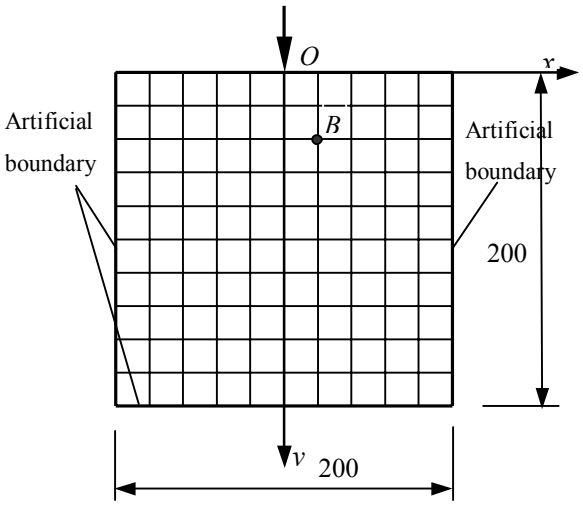

Fig. 2 The finite element model of example 1

In order to discuss the effect of coupling mass ρ_a on solid phase, the dimensionless solid phase displacement ($\xi = u/\rho k V_c$) of point B calculated by the analytical solution and the numerical solution at ρ_a=0 and ρ_a 0 are displayed in Fig.4 and Fig.5 respectively. From Fig.4 and

Table 1 Basic Material Properties (SI)

A	N	n	ρ_s	ρ_f	ρ	ρ_a	Q	R	k
1.902 ×10^7	2.746 ×10^7	0.467	4652	1346	3060	877	1.02 ×10^7	0.793 ×10^7	1.888 ×10^{-12}

Fig.5 we can see, the effect of ρ_a on solid phase is very small when the free surface is permeable. Because there is no solution of liquid phase displacements in the analytical method offered by Ref [12], this paper discusses the effect of coupling mass ρ_a on liquid phase displacements. Figure 6 presents for the dimensionless liquid phase displacements $\eta = U / \rho k V_c$ of the point B calculated with method presented in this paper versus $\tau = t / \rho k$ also with the free surface permeable. From Fig.6, we can obtain that at the initial stage the liquid displacements of ρ_a =0.0877×10^4 is relatively larger than that of ρ_a =0 when the free surface is permeable. With the growth of τ, the two kind of the liquid phase displacements tend to unanimity gradually, the effects of ρ_a are reduced accordingly.

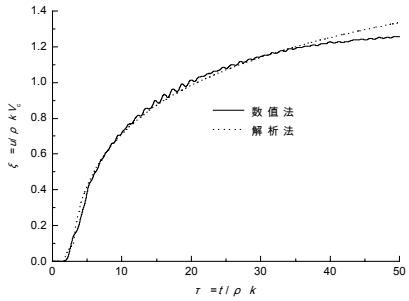

Fig. 3 Comparison of the solid phase displacement calculated by the analytical method with that calculated by numerical method

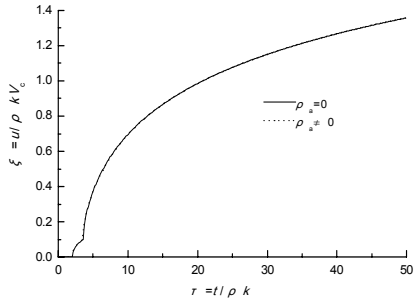

Fig. 4 Effect of coupling mass on solid phase displacement calculated by the analytical solution

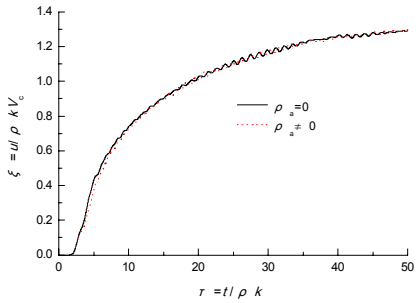

Fig. 5 Effect of coupling mass on solid phase displacement calculated by the numerical method

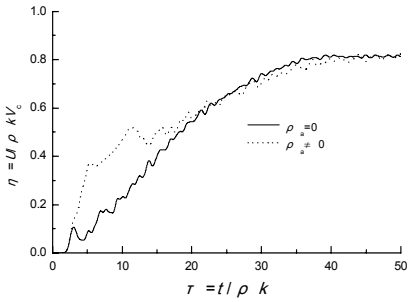

Fig.6 Effect of coupling mass on liquid phase displacement calculated by the numerical method

Example 2

The second example analyzed by the method presented in this paper is a rigid foundation with width 10m, on which is exerted a load $P = \sigma_0 \sin \omega t$, as shown in Fig.7. The effect of the load frequency *f* and coupling mass ρ_a on the dynamic responses of fluid saturated porous media is discussed now. The interface between the free surface of fluid saturated porous media and the contact face of rigid foundation should satisfy the following conditions: 1. The vertical displacements of each point on the contact surface of rigid foundation and the displacements of solid phase and liquid phase in each contact point are equal, namely $u_y = U_y$ .2. Without considering sliding of interface, so the displacements of solid phase at contact points are zero in horizontal direction, namely $u_x = 0$ .And the surface of the saturated porous media beyond the rigid foundation is assumed permeable.

From Fig. 8 ~10, taking $\tau = t/\rho k$ as the x-axis and $\xi = u/\rho k V_c$ as y-axis, the effects of coupling mass ρ_a on the vertical solid displacement of point A under three different frequencies f=1Hz, 2Hz,and 10Hz were presented. From these figures, we can see that the effects of the coupling mass ρ_a on the vertical solid displacement are very small, and the vertical solid displacement of ρ_a=0, is more than that of ρ_a=0.0877×10^4.

Fig. 11 ~ 14 presented the effects of ρ_a on the solid phase and liquid phase displacement at point B, C, D and E with frequency f=1Hz. In these figures, the y-axis are also the dimensionless displacement ($\xi = u/\rho k V_c$ or $\eta = U/\rho k V_c$). We can know from Fig. 11 ~14, it is same as example 1, ρ_a has not obvious effect on the displacements of the solid phase and has great effect on the displacements of the liquid phase. But there is a great difference form the example 1, the displacement of the liquid phase when ρ_a=0 is obviously greater than that when ρ_a=0.0877×10^4, while in example 1 the displacement of the liquid phase when ρ_a=0 is obviously smaller than that when ρ_a=0.0877×10^4. This must be because the rigid contact face leads to that the surface of the saturated porous medium contact with the rigid foundation can be partly seemed as impermeable boundary. The effects of ρ_a on the dynamic response of the saturated porous medium when the free surface is impermeable will be discussed next.

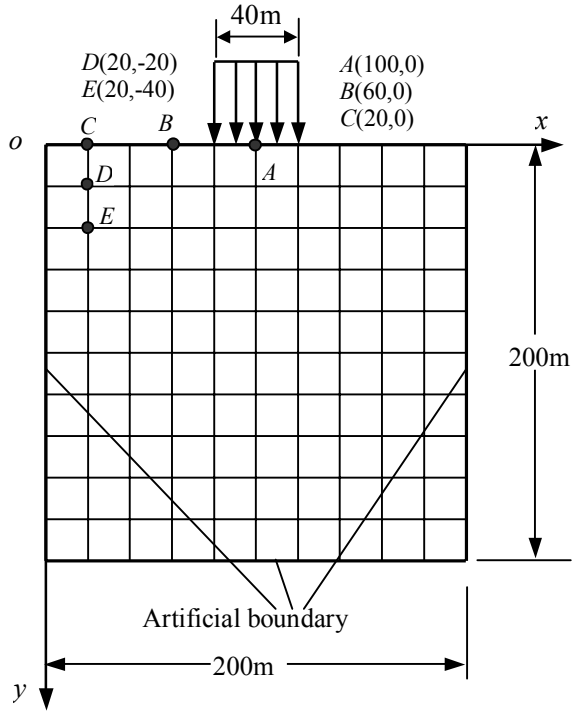

Fig.7 The finite element model of example 2

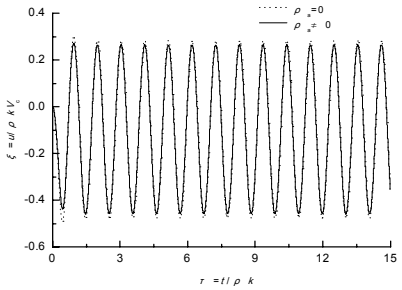

Fig. 8 Effect of coupling mass on the solid phase displacement of point A (f=1Hz)

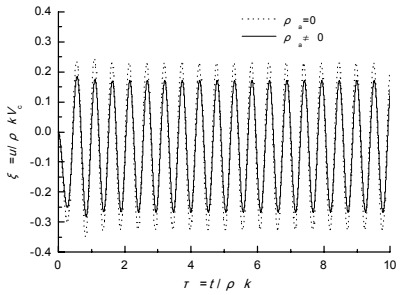

Fig. 9 Effect of coupling mass on the solid phase displacement of point A (f=2Hz)

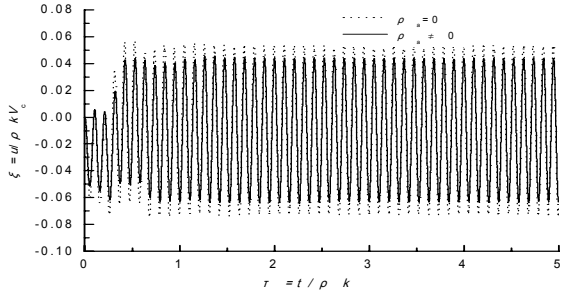

Fig. 10 Effect of coupling mass on the solid phase displacement of point A (f=10Hz)

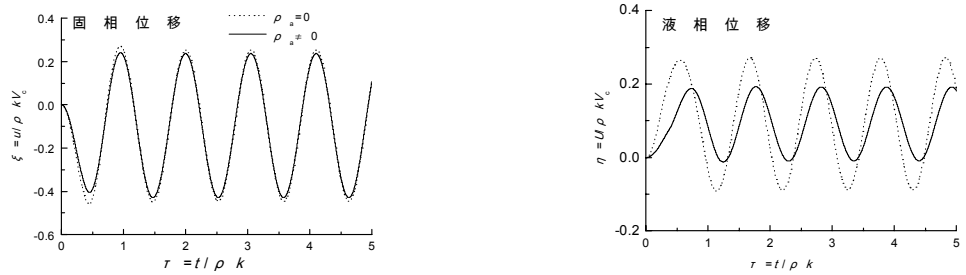

Fig. 11 Effect of coupling mass on the solid phase and liquid phase displacement of point B respectively

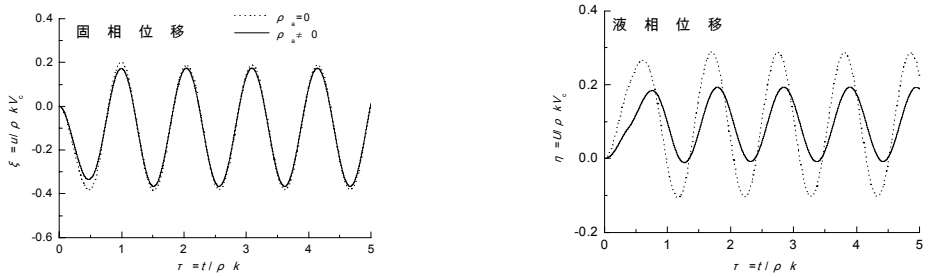

Fig. 12 Effect of coupling mass on the solid phase and liquid phase displacement of point C respectively

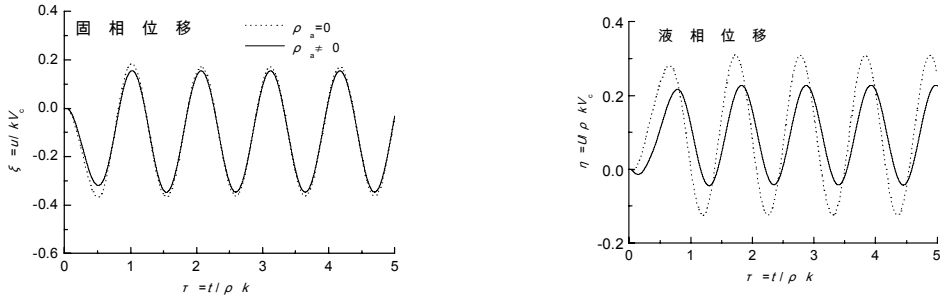

Fig. 13 Effect of coupling mass on the solid phase and liquid phase displacement of point D respectively

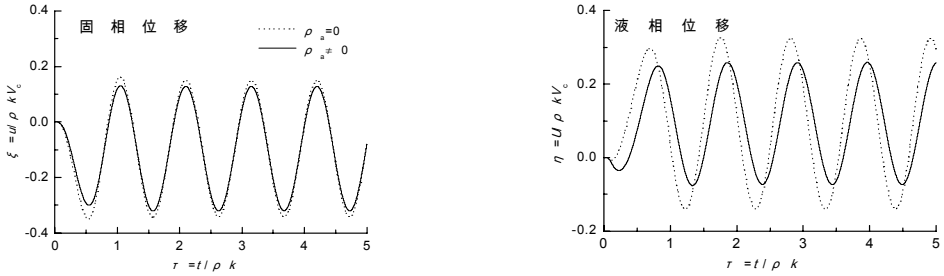

Fig. 14 Effect of coupling mass on the solid phase and liquid phase displacement of point E respectively

***Example* 3**

The above two examples are all assumed that the free surface is permeable -boundary, namely in free boundary (y =0), the pore water pressure is zero. Next, we will study the effect of coupling mass on the dynamic responses

of the saturated porous medium when the free surface is impermeable-boundary. The computational model adopted is the same as example 1 and the vertical concentrated staircase loads are applied in origin of coordinate. Because of the impermeable free surface, in origin of the coordinate, the stress on the solid skeleton should be 1-*n*, the pore water pressure is *n* (*n* is porosity), and on the surface, the vertical solid phase and lateral displacements are equal. Fig. 15 and Fig. 16 show the effect of coupling mass ρ_a on solid phase and liquid phase displacement of point B when the free surface is the impermeable and under the action of vertical concentrated staircase loads. In these two figures, the horizontal coordinates are also $\tau = t/\rho k$ and the vertical coordinates are the dimensionless solid phase displacements $\xi = u/\rho k V_c$ and liquid phase displacements $\eta = U/\rho k V_c$ of point B respectively. From the two figures, we can get a different conclusion from that of the permeable surface condition. That is, when the free surface is impermeable, the effects of ρ_a on the solid displacement and the liquid displacement are all apparent, and both of the solid and the liquid displacements when ρ_a=0.0877×10^4 is relatively small than that of ρ_a=0.With the growth of τ, the effects of ρ_a on the solid phase gradually increase. While the effects of ρ_a on the liquid phase are large in a given time quantum, beyond this time quantum, the effects of ρ_a on the liquid phase become weak.

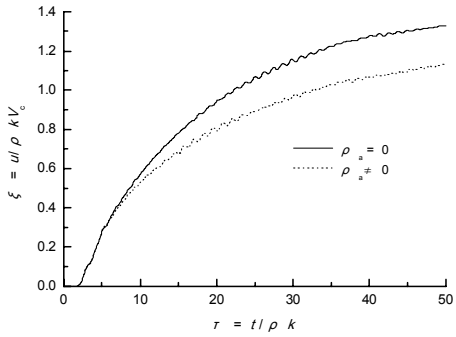

Fig. 15 Effect of coupling mass on solid phase displacement of the example 1 when the free surface being impermeable

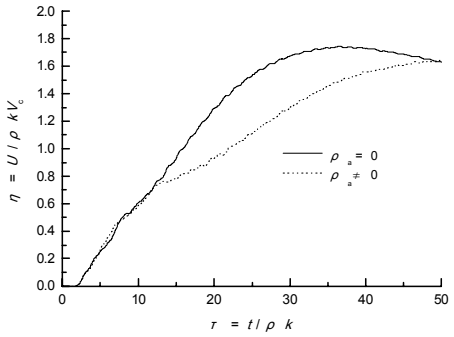

Fig. 16 Effect of coupling mass on liquid phase displacement of the example 1 when the free surface being impermeable

6. CLOSING REMARK

A high efficiency explicit finite element method for dynamic analysis of fluid saturated porous media considering of the coupling mass ρ_a are developed, and computing results of this method compared with analytic solution are presented in this paper. The computing results of two different loads indicate that the effects of the coupling mass on the dynamic responses of saturated porous medium are connected with the boundary condition of the free surface. When the free surface is permeable, the coupling mass has obvious effect on the liquid phase displacements while having little effect on the solid phase displacements, which can cause the diversification of pore pressure. And when the free surface is impermeable, the coupling mass has obvious effect both on the liquid phase displacements and the solid phase displacements. This stated method is of a very effective method with the characteristic of high calculating speed and small memory needed, and offering an effective method for dynamic response numerical simulation of fluid saturated porous media.

REFERENCES

[1] M. A. Biot. (1956). Theory of elastic wave in fluid-saturated porous solid. *The Journal of the Acoustical Society of America* **28**:168-178

[2] J.Ghaboussi and E.L. Wilson. (1972). Variational formulation of dynamics of fluid saturated porous elastic solids. *Journal of Engineering Mechanics Division, ASCE* **98**:947-963.

[3] O.C. Zienkiewicz, A.H.C. Chan, M. Pastor, and B.A. Schrefler. 1999Computational Geomechanics-with special reference to earthquake engineering, West Sussex of England: John Wiley & Sons Ltd,.

[4] O.C. Zienkiewicz, et al. (1984). Dynamic behavior of saturated porous media: the generalized Biot formulation and its numerical solution. *International Journal of Numerical and Analytical Method in Geomechanics* **8:**71-96

[5] J.H. Prevost. (1985). Wave propagation in fluid-saturated porous media: an efficient finite element procedure. *Soil Dynamics and Earthquake engineering* **4**:183-201

[6] D. Aubry, Computational soil dynamics and soil-structure interaction. Development in dynamic soil-structure interaction, P.Gülkan and R.W.Clough, Eds. 1993. 43-60.

[7] Yuan Di and Tadanobu Sato. (2003). Liquefation analysis of saturated soils taking into account variation in porosity and permeability with large deformation. *Computers and Geotechnics* **30**: 623-635.

[8] Zhao Chenggang, Li Weihua et al. (2005). An explicit finite element method for Biot dynamic formulation in fluid-saturated porous media and its application to a rigid foundation. *Journal of Sound and Vibration* **282:5**, 1155-1168.

[9]Zhao Chenggang, Li Weihua et al. (2005). An explicit finite element method for dynamic analysis in three-medium coupled systems and its application. *Journal of Sound and Vibration* **282:5**, 1169-1181.

[10] Liao Zhenpeng, et al. (1984). A Transmitting boundary for transient wave analyses. *Science in China (A)* **27**: 1063~1076.

[11] J.Chen. (1994). Time domain fundamental solution to Biot complete equations of dynamic poro-elasticity Part I: two-dimensional solution. *Int. J. Solids Structures* **31:10**, 1447~1490.